Passivity Based Control Of Stewart Platform For Trajectory Tracking

Mr Tariku Sinshaw, Addis Ababa Institute of Technology, School of Electrical and Computer Engineering, Addis Ababa, Ethiopia.

Abstract- Passivity based control, as one of the tools available to design robust controllers, is introduced for trajectory tracking of the Stewart platform. Since Passivity is a fundamental property of many physical systems which may be roughly defined in terms of energy dissipation and transformation, its inherent input output property quantifies and qualifies the energy balance of a system when simulated by external inputs to generate some outputs. PD+ controller is designed based on passivation principle so that the closed loop system becomes globally uniform and asymptotically stable.

The mathematical model of the Stewart platform, derived from Euler Lagrange equations of motion, is simulated on MALAB/Simulink with the designed controller. So as to get the desired leg-length trajectory, the inverse kinematics formulation is investigated. The mathematical model is verified using "automatic dynamic analysis of mechanical systems" (ADAMS) software.

In the absence of disturbances, the maximum trajectory tracking error is recorded as $0.006m$ in the time interval between 0sec and 0.8sec. Applying unit step disturbance makes the error $0.006m$ after 0.8sec, which never be seen in undisturbed system.. The maximum speed of all the six legs trajectory have been found to be $0.43m/s$, $0.49m/s, 0.48m/s$, $0.5m/s$, $0.5m/s$ and $0.49m/s$ respectively. More realistic results are observed from ADAMS simulation results.

Key words: passivity based control, PD+, global uniform asymptotically stable, Euler Lagrange equation, ADAMS software, inverse kinematics, MATLAB/Simulink.

I Introduction

Unlike open-chain serial robots, parallel manipulators are composed of closed kinematic chains. Serial manipulators can be defined as simple kinematic chains for which all the connection degrees are two, except for the base and the end effectors, such a chain is called an open loop kinematic chain. A closed-loop kinematic chain is obtained when one of the links, but not the base, possesses a connection degree greater than or equal to three, there exist several parallel kinematic chains between base platform and the moving platform. [1]

Serial robots consist of a number of rigid links connected in series so that every actuator supports the weight of the successor links. This serial structure suffers from several disadvantages such as low precision, poor force exertion capability and low payload-to-weight-ratio. Under heavy loads, serial robots cannot perform precision positioning and oscillate at high-speeds. [4]

On the other hand, in parallel manipulators the load is shared by several parallel kinematic chains. This superior architecture provides high rigidity, high payload-to-weight-ratio, high positioning accuracy, low inertia of moving parts and a simpler solution of the inverse kinematics equations over the serial ones. Since high accuracy of parallel robots stems from load sharing of each actuator, there are no cumulative

joint errors and deflections in the links. Furthermore, the positioning accuracy of parallel robots is high due to the fact that the positioning error of the platform cannot exceed the average error of each leg's positions. They can provide nanometer-level motion performance. But they have smaller workspace and singularities in their workspace. [4]

Since a parallel structure is a closed kinematics chain, all legs are connected from the origin of the tool point by a parallel connection. This connection allows a higher precision and a higher velocity. Parallel kinematic manipulators have better performance compared to serial kinematic manipulators in terms of a high degree of accuracy, high speeds or accelerations and high stiffness. Therefore, they seem perfectly suitable for industrial high-speed applications, such as pick-and-place or micro and high-speed machining. They are used in many fields such as flight simulation systems, manufacturing and medical applications. [3]

One of the most popular parallel manipulators is the general purpose 6 degree of freedom (DOF) Stewart Platform (SP) proposed by Stewart in 1965 as a flight simulator. It consists of a top plate (moving platform), a base plate (fixed base), and six extensible legs connecting the top plate to the bottom plate. SP employing the same architecture of the Gough mechanism is the most studied type of parallel manipulators. This is also known as Gough–Stewart platforms in literature. [3]

While the kinematics of parallel manipulators has been studied extensively during the last two decades, fewer contributions can be found on the dynamics of parallel manipulators. Dynamical analysis of parallel robots, which is very important to develop a model-based controller, is complicated because of the existence of multiple closed-loop chains. Different modeling approaches have been illustrated by different researchers. Euler-Lagrange method, virtual work principles, Lagrange formulation and analyzing using screw theory were used for the modeling of robot manipulators. Dynamic equations of a Stewart-Gough platform can be derived based on Lagrange's formulation. [4]

The term passivity based control (PBC) was coined in 1989 in the context of adaptive control of robot manipulators to define a controller methodology whose aim is to render the closed loop system passive. This objective seemed very natural within that context, since the robot dynamics defines a passive map from input torque to output link velocities. As a matter of fact passivity property is inherent to many other physical systems such as electrical and electromechanical. [8]

II The Stewart Manipulator

The Stewart platform is six degrees of freedom robot. It is composed of six prismatic legs connected to the base and moving platform by passive spherical joints and at the middle of these legs are prismatic actuated joints. The design variation of different Stewart platform types dependents only on the placements of the joint on the base and the platform. The figures below are used to classify these different design types. [9]

Figure 1: solid model of typical Stewart platform manipulator [10]

III Kinematics of the Stewart Platform

For the analysis of the kinematics of the Stewart manipulator, we need to have the rotation matrix and the position vector.

The first rotation (yaw) around z axis, $R_z(\gamma)$

$$R_z(\gamma) = \begin{bmatrix} c\gamma & -s\gamma & 0 \\ s\gamma & c\gamma & 0 \\ 0 & 0 & 1 \end{bmatrix} \quad (1a)$$

The second rotation (pitch) around y axis, $R_y(\beta)$

$$R_y(\beta) = \begin{bmatrix} c\beta & 0 & s\beta \\ 0 & 1 & 0 \\ -s\beta & 0 & c\beta \end{bmatrix} \quad (1b)$$

The third rotation (roll) around x axis, $R_x(\alpha)$

$$R_x(\alpha) = \begin{bmatrix} 1 & 0 & 0 \\ 0 & c\alpha & -s\alpha \\ 0 & s\alpha & c\alpha \end{bmatrix} \quad (1c)$$

The rotation matrix, ${}^{T}_{B}R$, of the end effector referred to the base frame is the product of the individual rotation matrices given in equation (1a), (1b) and (1c).

$${}^{T}_{B}R = R_z(\gamma)\, R_y(\beta)\, R_x(\alpha) =$$

$$\begin{bmatrix} c\beta c\gamma & c\gamma s\alpha s\beta - c\alpha s\gamma & s\alpha s\gamma + c\alpha c\gamma s\beta \\ c\beta s\gamma & c\alpha c\gamma + s\alpha s\beta & s\gamma c\alpha s\beta s\gamma - c\gamma s\alpha \\ -s\beta & c\beta s\alpha & c\alpha c\beta \end{bmatrix} \quad (2)$$

Where,$\{S(.) = \sin(.)$ and $C(.) = \cos(.)\}$

And the position will be;

$$P = [P_x \quad P_y \quad P_z]^T \quad (3)$$

With three positions, p_x, p_y and p_z

The length of the i^{th} legs/links for the Stewart platform with six legs is expressed in equation (4) with upper connecting point, GT_i and lower connecting point, B_i

$$L_i = {}^{T}_{B}RGT_i + P - B_i, i = 1.....6 \quad (4)$$

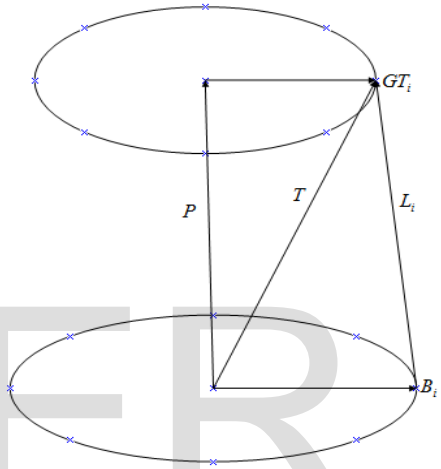

Figure2: kinematic diagram for determination of leg length

IV Trajectory Tracking of the Stewart Platform

In order to move the robot along a specified path, a trajectory planning algorithm will be developed. Kane's transition function is used for trajectory planning algorithm of the Stewart platform.

$$Y(t) = y_0 + (y_f - y_0)\frac{t - t_0}{t_f - t_0} - \frac{y_f - y_0}{2\pi}\sin(2\pi\frac{t - t_0}{t_f - t_0}) \quad (5)$$

Where y (t) is the position function, y_0 is the initial position y_f is the finish position; *t* is time, t_0 is initial time and t_f *is* the finish time.

V Dynamics of the Stewart Platform

The EL formulation is particularly suited for passivity based control (PBC) since it underscores the role of the interconnections between systems and provides us with the storage and dissipation functions, which are the corner stone of the PBC design technique. Therefore, it is better to use EL method to derive the dynamic modeling of the SP manipulator.

$$\frac{d}{dt}\frac{\delta L}{\delta \dot{q}} - \frac{\delta L}{\delta q} = \frac{d}{dt}\left(\frac{\delta K(q,\dot{q})}{\delta \dot{q}}\right) - \frac{\delta K(q,\dot{q})}{\delta q} + \frac{\delta P(q)}{\delta q} = \tau \tag{6}$$

Where, L is the Lagrange function and given by:

$$L = K(q,\dot{q}) - P(q) \tag{7}$$

Where, K(q,q̇) is the kinetic energy and P(q) is the potential energy.

From Equation (6) the dynamics of the Stewart manipulator can be rewritten as:

$$M(q)\ddot{q} + V(q,\dot{q})\dot{q} + G(q) = \tau \tag{8}$$

Where, M(q) is inertia matrix of the manipulator, V(q,$\dot{q}$) is the coriolis/centrifugal vector, G(q) is the gravity matrix of the manipulator, τ is the actuator force and q is the generalized coordinate given by $L = [L_1, L_2, L_3, L_4, L_5, L_6]$ where, L is the leg length.

$\tau = [\tau_1 \ \tau_2 \ \tau_3 \ \tau_4 \ \tau_5 \ \tau_6]$ are the actuator forces applied by the actuattor in the six legs of the Stewart manipulator.

VI Dynamics of Actuators

The leg system of the Stewart platform is composed of dc motor, precision linear bearing & ball screw and coupling elements.

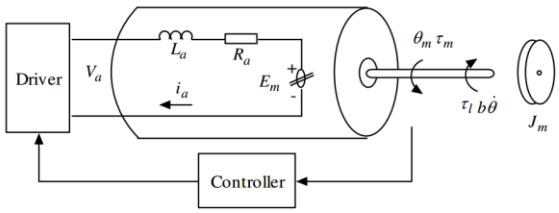

Figure 3: Circuit diagram of the DC motor

The symbols represent the following variables; θ_m is the rotor position (radian), τ_m is the produced torque by the motor (Nm), τ_l is the load torque, V_a is the armature voltage (V), L_a is the armature inductance (H), R_a is the armature resistance (Ω), E_m is the reverse EMF (V), k_b is the reverse EMF constant, k_T is torque constant.

From figure 3, the armature current can be written as:

$$I_a = \frac{V_a - k_b\omega}{R_a + L_a s} \tag{9}$$

And also the angular speed of the motor can be expressed as:

$$\left\{\begin{array}{l} J_m s\omega + b_m\omega + \tau_L = k_T I \\ \omega = \dfrac{k_T I - \tau_L}{J_m s + b_m} \end{array}\right\} \tag{10}$$

VII Controller Design

a) Parameters Setting of the Stewart Platform

To make sure the performance of the controller designed for the system, all parameters of the stewart platform should be specified. Parameters like, attachement points on the moving platform, attachement points on the base platform, stewart plaatform constants and DC motor constants are set to a specified value.

b) Design of PD+ Controller

PD+ controller on the basis of the passivity properties of the EL system, which mainly focuses on the conservation of energy, is designed.

PD controller will be used for set point regulation of Stewart platform. It concerns the global asymptotic stabilization via energy shaping plus damping injection of the equilibrium $[q,\dot{q}]^T = [q^*,0]^T$, with q^* a constant vector,

Consider the equation below:

$$M(q)\ddot{q} + V(q,\dot{q})\dot{q} + G(q) = u \qquad (11)$$

Equation (11) describes the dynamics of the system with **u** as a control vector.

Let the state-feedback control law be given as:

$$u = -\frac{\delta V_C(q)}{\delta q} - \frac{\delta F_C(\dot{q})}{\delta \dot{q}} \qquad (12)$$

The function $V_C(q)$ is such that the potential energy of the closed loop system $V_d(q) = V(q) + V_C(q)$ has unique global minimum at $q = q*$. And the dissipation function, $F_C(\dot{q})$ satisfies $\frac{\delta F_C(\dot{q}=0)}{\delta \dot{q}} = 0$ and $\dot{q}^T \frac{\delta F_C(\dot{q})}{\delta \dot{q}} > 0$ for all $\forall q \neq 0$.

Natural candidate for new potential energy function is then:

$$V_d(q) = \frac{1}{2} K_P \tilde{q}^2 \qquad (12)$$

Where, $k_P > 0$ and $\tilde{q} = q - q^*$.

Similarly, the desired Rayleigh dissipation functions can be chosen as:

$$F_d(\dot{q}) = \frac{1}{2} K_d \dot{q}^2 \qquad (13)$$

Where, $K_d > 0$

These choices lead to the control:

$$u = \frac{\delta(V(q) - V_d(q))}{\delta q} - \frac{\delta F_C(\dot{q})}{\dot{q}}$$

$$\equiv g(q) - K_P\tilde{q} - K_d\dot{q} \qquad (14)$$

There are two positive definite constants, K_P and K_d, and the gravity matrix component $g(q)$. In the designed controller, there is gravity cancellation.

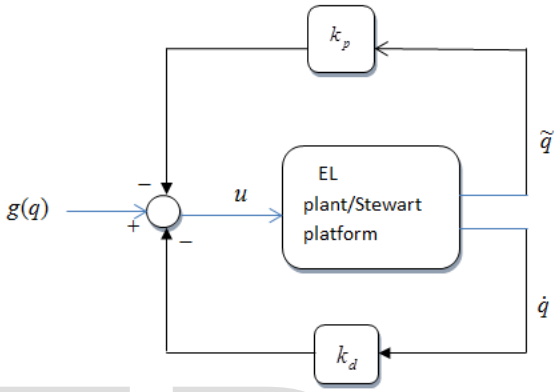

Figure 4: PD controller for set point regulation

The PD+ controller, the natural extension of PD controller to tracking control, is one of the first results guaranteeing global tracking for rigid- joint robots that is global uniform asymptotic stability (GUAS) of the origin $(\tilde{q},\dot{\tilde{q}}) = (0,0)$.

Therefore, the whole system with the PD+ controller with k_p (proportional constant) and k_d (derivative constant) will be expressed as follows.

$$M(q)\ddot{q} + V(q,\dot{q})\dot{q} + G(q) = -K_P\tilde{q} - K_d\dot{q} \qquad (15)$$

c) ADAMS modeling of Stewart platform

The four step process used in combining MATLAB controls with the Stewart platform in ADAMS are; build the ADAMS model, identify the ADAMS inputs and outputs and export to the plant model, build the control system block diagram and simulate the model respectively.

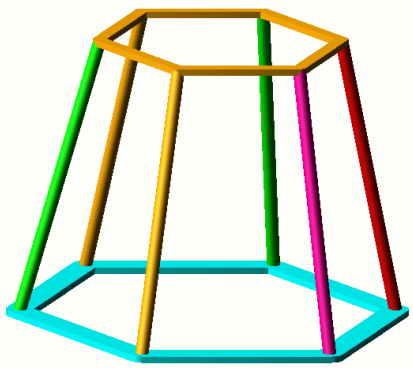

Figure 5: ADAMS model of Stewart platform

The components of figure 5 are geometric links (six links on the upper platform, six links on the upper leg, six links on the lower leg, six links on the base platform), Connectors (twelve spherical and 6 prismatic type connectors), forces (the force generated by the six prismatic type connectors in each legs).

The final setup of the Simulink simulation after exporting the ADAMS model is shown in figure 6.

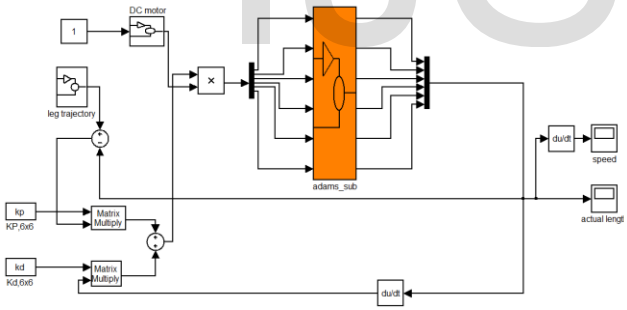

Figure 6: ADAMS model and Simulink control

VIII Results

a) Performance Analysis of Outer Loop

The initial values of position and orientation, as well as the leg lengths are given as follows:

$$x = 0m,\quad y = 0m,\quad z = 0.21m \quad \text{and} \quad \alpha = \beta = \gamma = 0(rad)$$

Andalso, $L_1 = L_2 = L_3 = L_4 = L_5 = L_6 = 0.22m$

We need to represent the unmodelled joints of the stewart platform with unit step disturbances and let's observe the effects on the performances of the system.

Case1: static reference

$$x = 0.07m,\quad y = 0.06m,\quad z = 0.05m \quad \text{And} \quad \alpha = \beta = \gamma = 0(rad)$$

For the listed reference positions and orientations set point values as input for the inverse kinematic algorithm, lets observe the values of all the six leg lengths with in the specified time range ($0 \rightarrow 1\text{sec}$) with the addition of unit step disturbances.

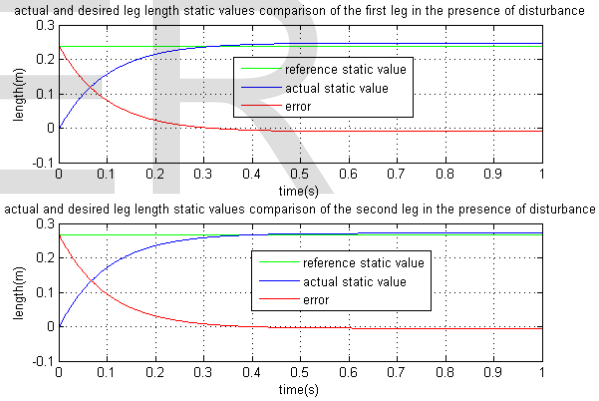

(a)

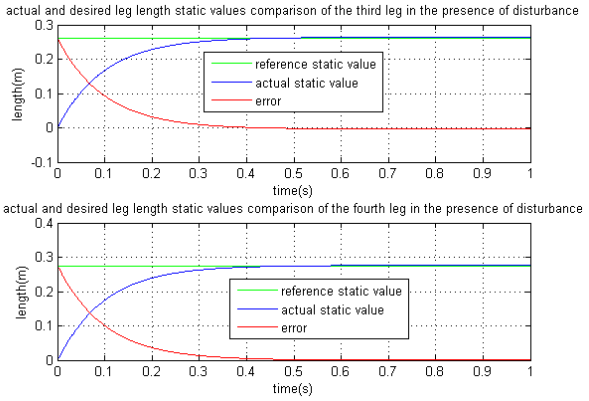

(b)

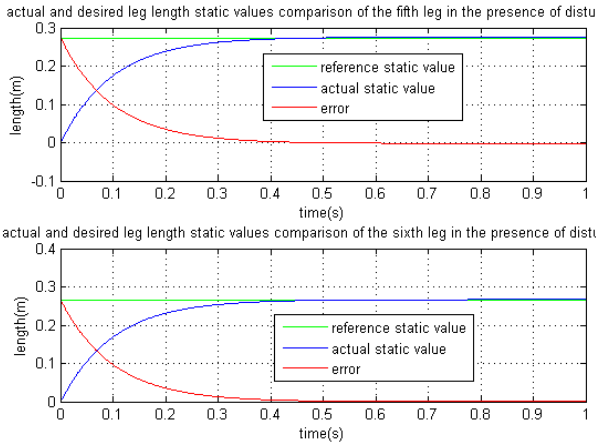

(c)

Figure 7: comparison of desired and actual leg length set values in the presence of unit step disturbances (a) first and second leg, (b) third and fourth leg, (c) fifth and sixth leg

Case2: trajectory reference

$$\begin{bmatrix} x = 0.035t - 0.01\sin(\pi t) \\ y = 0.03t - 0.01\sin(\pi t) \\ z = 0.025t - 0.01\sin(\pi t) \end{bmatrix} m \quad \text{And}$$

$$\begin{bmatrix} \alpha = 0.08t - 0.03\sin(\pi t) \\ \beta = 0.13t - 0.04\sin(\pi t) \\ \gamma = 0.17t - 0.05\sin(\pi t) \end{bmatrix} (rad)$$

For the listed reference positions and orientations trajectories as input for the inverse kinematic algorithm, lets observe the trajectories of all the six leg length and velocities with in the specified time range $(0 \rightarrow 1\text{sec})$ in the presence of unit step disturbance.

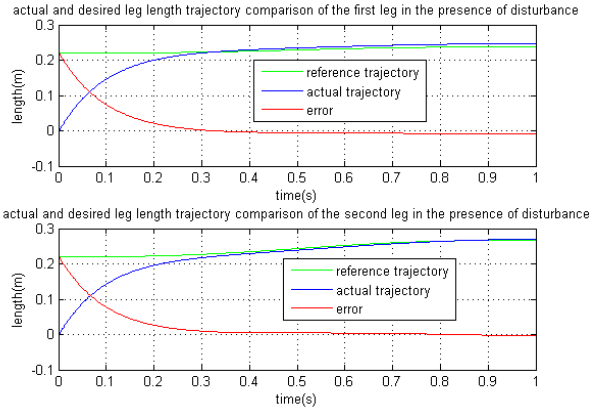

(a)

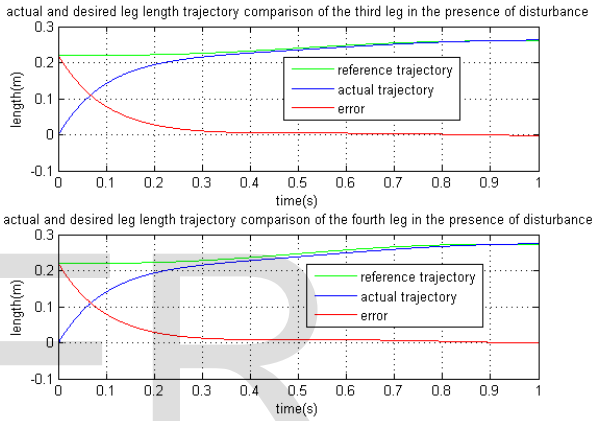

(b)

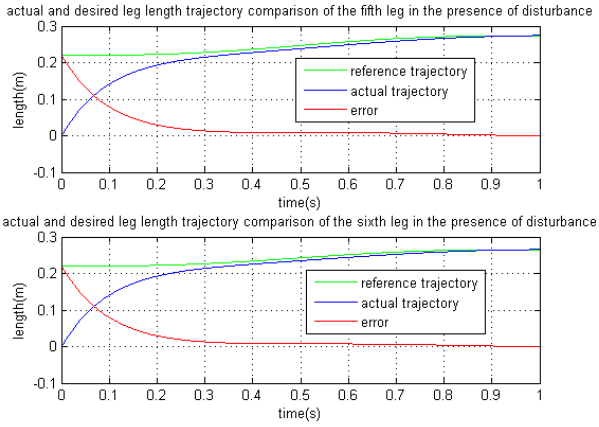

(c)

Figure 8: comparison of desired and actual leg length trajectories in the presence of disturbances (a) first and second leg, (b) third and fourth leg, (c) fifth and sixth leg

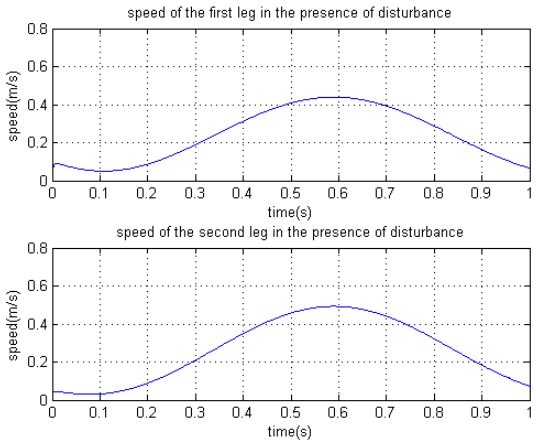

(a)

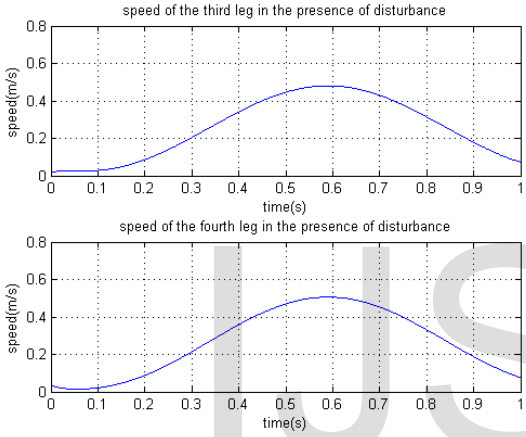

(b)

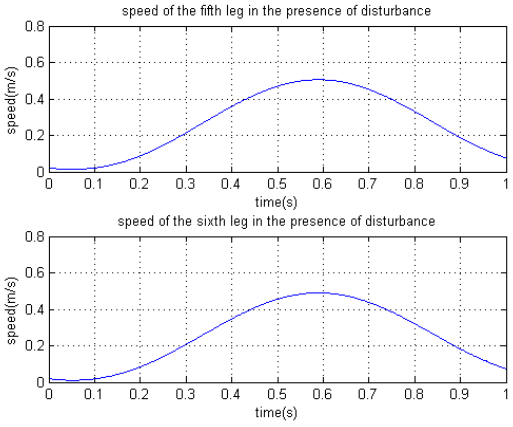

(c)

Figure 9: speed of legs motions in the presence of disturbances (a) first and second leg, (b) third and fourth leg, (c) fifth and sixth leg

From figure 7, in all the six legs, the system tracks the set point value at 0.4sec after some delay. As the time goes from 0sec to 0.4sec, the error decreases and finally becomes approximately zero at 0.4sec.

From figure 8, in all the six legs, the system tracks its initial leg lengths value at 0.3sec. The desired trajectory with error of $0.006m$ in the time interval between 0.3sec and 0.8sec, and approximately zero errors after 0.8sec is achieved.

In figure 9, the motion starts and finishes with nonzero velocity in all the six legs, this is due to limitation of mathematical modeling and it is verified using ADAMS simulation results presented in the next section. The maximum speed is achieved at 0.6sec in all the legs and have the value of $0.43m/s, 0.49m/s, 0.48m/s, 0.5m/s,$ $0.5m/s$ and $0.49m/s$ from the first to the sixth leg respectively.

b) ADAMS simulation results

Taking 'case 2 – trajectory reference' as an input.

The ADAMS simulation generated leg length trajectories as shown in *figure 11* by taking reference leg length trajectories from *figure 10*.

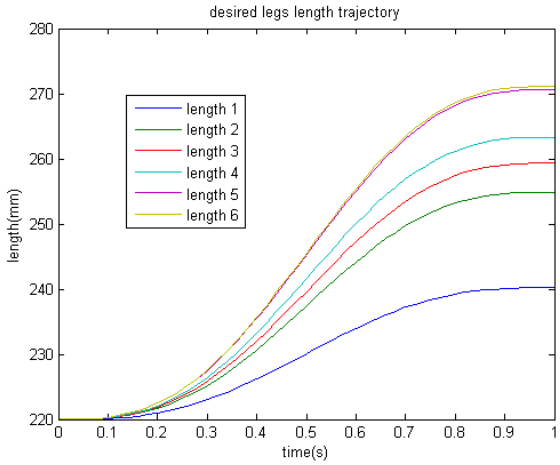

Figure 10: desired length trajectories of the six legs

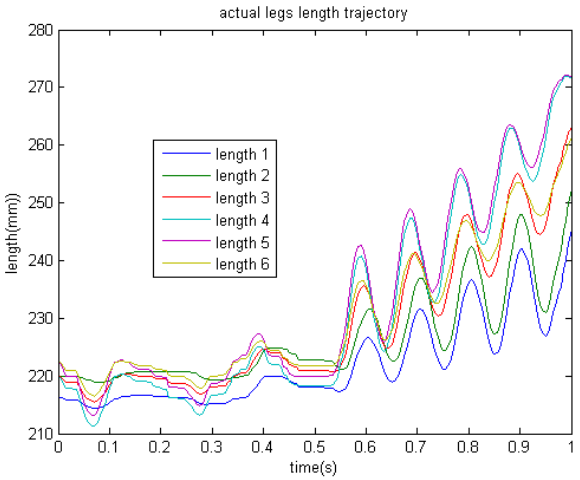

Figure 11: actual length trajectories of the six legs

The deviation/error of the leg lengths trajectory is shown in figure 12. As the figure clears, almost similar error characteristics is observed in the time interval between 0sec and 0.5sec. After 0.5sec , the error expands due to sensors (used in each of the links) problem. At 1sec, The errors are minimized except the first leg (the upper link of the leg gets inserted to the lower link of the leg) as a result of failure of the sensor (which can't take action when the leg length becomes below the minimum leg length accurately) used in the link.

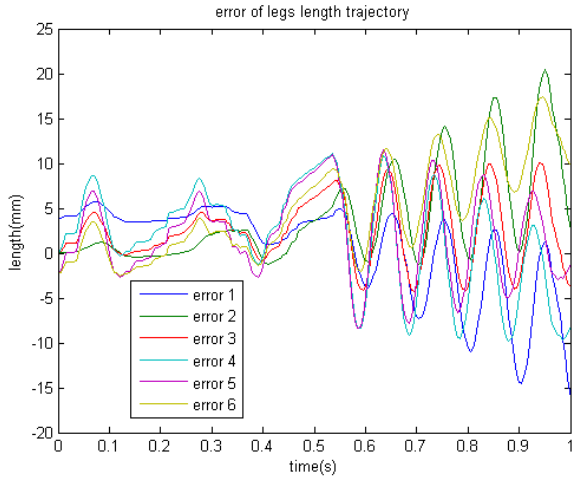

Figure 12: trajectory errors of the six legs

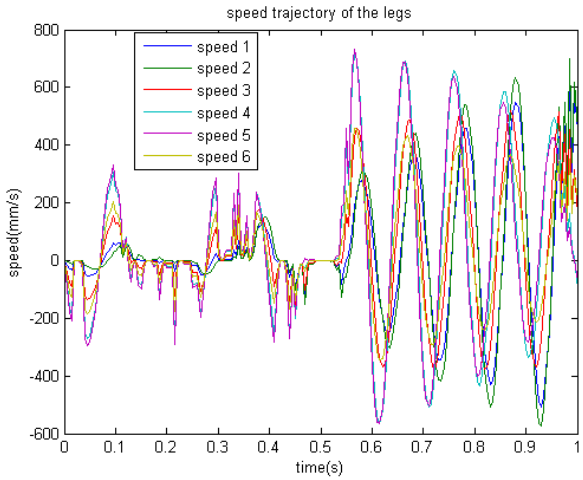

Figure 13: speed trajectory of the six legs

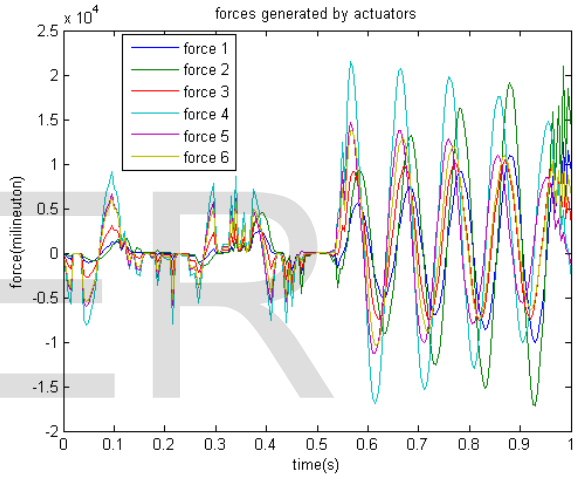

Figure 14: actuator forces

The actuator forces are also calculated by the controller designed in MATLAB/Simulink and presented in figure 14, which is bounded from below (-15N) and above (22N). As shown from figure 13, the motions start and finish with zero velocity, and have a non-zero trajectory otherwise.

As can be seen from the ADAMS simulation result, the leg length trajectories possess a certain oscillation pattern, and this is due to friction, link and joint flexibility and other factors, since ADAMS model represent the physical model of the system.

IX conclusions

The PD+ controller, PD controller with gravity compensation, guaranteed tracking for rigid joint robots in the sense of global uniform asymptotic stability (GUAS). The control law is designed in order not to have the gravity term cancelation.

The simulation result shows the effect of the controller on the performance of the system. In the absence of disturbances, the maximum trajectory tracking error is recorded as $0.006m$ in the time interval between $0\sec$ and $0.8\sec$. Applying unit step disturbance makes the error $0.006m$ after $0.8\sec$ which never be seen in undisturbed system. The maximum speed from the initial position to final position is recorded as $0.43m/s, 0.49m/s, 0.48m/s, 0.5m/s, 0.5m/s$ and $0.49m/s$ from the first to the sixth leg respectively.

The ADAMS simulation results show the real time performance of the system, having some difference with mathematically modeled results. From the simulation studies, one can generalize that the system meets the desired output.

Finally the stability of the overall system is checked on the basis of lyapunov's direct method, and it is observed that the system is globally uniformly asymptotically stable.

x References

[1] *Richard M. Murray, 'Mathematical Introduction to Robotic Manipulation', University of California, Berkeley, 1994*

[2] *Neil Munro, Ph.d., D.sc. 'Robot Manipulator Control Theory and Practice', second edition, University of Manchester Institute of Science and Technology Manchester, United Kingdom.*

[3] *Serdar Küçük, 'serial and parallel robot manipulators – kinematics, dynamics, control and optimization', 2012*

[4] *A. Ghobakhloo, M. Eghtesad and M. Azadi, "Position Control of a Stewart Gough Platform Using Inverse Dynamics Method with Full Dynamics", IEEE publication, 2006.*

[5] *D.Stewart, "review of stewart platforms, chapter 1".*

[6] *Nawal Azoui, Lamir Saidi,"passivity based adaptive control of robotic manipulators electrically controlled", international journal of sciences and technology, Vol. 34, 2011.*

[7] *Houssem Abdellatif, Jens Kotlarski, Tobias Ortmaier and Bodo Heimann, "Practical Model-based and Robust Control of Parallel Manipulators Using Passivity and Sliding Mode Theory".*

[7] *Romeo Ortega, Antonio Loria, Per Johan Nicklasson and Hebertt Sira-Ramfrez, 'Passivity-based Control of Euler-Lagrange Systems', Mechanical, Electrical and Electromechanically Applications.*

[7] *Anders Lohmann MadsenMadsen, "design of Stewart platform for wave compensation", master's thesis, 2012.*

[7] *Assoc. Prof. Dr Mohamad Kasim Abdul Jalil, design and development of 6-dof motion platform for vehicle driving simulator, Faculty of Mechanical Engineering, Universiti Teknologi Malaysia*

Autor Profile

Mr. Tariku sinshaw (Msc in control engineering.)
Lecturer at Debremarkos University
Department of Electrical and Computer Engineering
Email: tareelectr@gmail.com
Tel: (+) 251-930-074749
Ethiopia